

FABRICATION OF A DISORDERED AND NANO-GRAIN SIZED FeAl INTERMETALLIC ALLOY BY TWO BALL MILLING CONDITIONS: MICROSTRUCTURAL CHARACTERIZATION AND CRYSTALLITE MODELING PERSPECTIVE

R. A. RODRÍGUEZ-DÍAZ^a, JUAN FRAUSTO-SOLIS^{a*}, A. SEDANO^b, A. MOLINA^b, J. PORCAYO-CALDERÓN^b, J. JUAREZ-ISLAS^c

^aUniversidad Politécnica del Estado de Morelos, Boulevard Cuauhnahuac 566, Col. Lomas del Texcal, 62574 Jiutepec, Morelos México

^bCentro de Investigación en Ingeniería y Ciencias Aplicadas, UAEM, Av. Universidad 1001, Col. Chamilpa, Cuernavaca Mor., México.

^cInstituto de Investigaciones en Materiales-UNAM, circuito exterior S/N, Ciudad Universitaria, C. P. 04510, México DF, México.

In this work a disordered Fe₄₀Al (at. %) alloy was prepared by the low energy ball milling technique from a stoichiometric mixture of high purity powders of Fe and Al, using different milling times. The ball milling process was performed by using two ball weight / sample weight ratios of 8:1 and 4:1. A Fe₄₀Al alloy with a disordered cubic B2 type crystal structure was synthesized at 20 h of milling process when using a ball weight to powder weight ratio of 8:1. The crystallite size corresponding to FeAl phase was reduced as the milling time elapsed while its lattice parameter showed a tendency to increase as the milling time advanced. In the same way the lattice strain was increased with the advance of milling process. Finally optimization methods applied for determine the best parameters of this process are discussed.

(Received March 26, 2015; Accepted May 29, 2015)

Keywords: Ball milling, FeAl Alloy, Intermetallic Compound, Microstructural Characterization

1. Introduction

The FeAl intermetallic compounds are increasingly attractive as engineering materials because of their excellent physical, chemical and mechanical properties, besides that these materials have a low density and good resistance to corrosion and oxidation at ambient and elevated temperature [1-2]. Recent studies have demonstrated the ease of preparing FeAl Intermetallic compounds by powder metallurgy (PM) processes involving hot isostatic pressing [3], extrusion [4], forging or hot pressing [5] and injection molding powders. FeAl powders used for the processes of MP were generally prepared by mechanical alloying (MA) [3]. Several investigations have been developed in order to improve the ductility of the Fe-Al intermetallic compounds, as a result of these studies, it can be concluded that the following strategies induce a significant improvement of the deformation behavior of these alloys: removal of the excess of crystal vacancies [6, 7], increasing the cohesive strength of the grain boundaries [8, 9], grain refinement [10, 11], microstructure control achieved by thermo-mechanical processing [12] and also by reducing the degree of long range order and decreasing the size of nano-metric grains [13, 14]. MA is among of the better promising processing methods that have been rapidly evolving and has been used to produce alloys and metal oxides that are difficult or impossible to elaborate by

*Corresponding author: juan.frausto@upemor.edu.mx

conventional processing methods. Besides, MA processing technique is able to produce nanocrystalline materials [15]. In previous researches, it was observed a significant enhancement in some mechanical properties, as a result of the refinement of microstructure, nanometric grains were obtained, and also to a dispersion strengthening mechanism induced by the MA process [16, 17]. MA is a high energy ball milling process, the MA is a solid state processing technique for the synthesis of a variety of equilibrium and non-equilibrium phases and phase mixtures. Mechanical alloying has also been successfully utilized in order to extend the solid solubilities in many commercially important alloy systems. Many intermetallic compounds which have high melting points and are difficult to elaborate by conventional processing techniques, could be simply synthesized with a homogeneous structure and composition by MA [18]. In addition, AM process technique is able to produce a disordered crystalline structure, which constitutes a microstructural characteristic that are desired to obtain better mechanical properties and particularly the deformation behavior of the intermetallic FeAl alloys. It is well known that partially ordered phases are stronger than those which are completely disordered or totally ordered (this is because at a certain value of the long-range order parameter, S , the super-dislocations are separated into unlinked singles) [19]. With the process of mechanical alloying has been successfully synthesized systems Fe-Al with different compositions and have been shown to have formed various phases, depending on the milling conditions [20-22]. Some previous investigations have reported the production of Fe-Al based alloys with nano-metric size grain under different experimental conditions [23-25]. However, the microstructure and mechanical behavior of the alloys produced by AM are greatly dependent on the conditions of ball milling technique involved in the powder metallurgy (PM) processing route [23-25]. Therefore, an increasingly systematic research is required to correlate the conditions of processing with the microstructure and properties. In this paper the influence of two milling conditions at low energy on the synthesis and subsequent microstructural characterization of the alloy powder was studied Fe₄₀Al.

2. Materials and Methods

Metallic powders of Al and Fe of high purity analytical grade 99.9% were mixed at a ratio of Fe₆₀Al₄₀ (at.%), and placed inside a vial with balls, both made of agate compound. The powder mixture was sprayed with a process control agent consisting of analytical grade ethyl alcohol in an amount of 0.002 ml / g of the weight mixture of Fe and Al. Subsequently, the powder mixture was encapsulated within the agate vial under a nitrogen atmosphere. And in this way proceed with the mechanical milling of the ample in a low-energy planetary mill (Fritsch Pulverisette) using a rotation speed of 300 rpm and the two ratios (ball weight / sample weight) 8:1 and 4:1. The technique of scanning electron microscopy (SEM) was used in order to characterize the evolution of size and morphology as well as the chemical homogeneity of the powders used in the process of mechanical milling as the milling time elapsed. Microstructural characterization was performed in a SEM mark Estereoscan 440 connected to a silicon detector with window of beryllium (mark Oxford Pentafel) with a resolution of 163 eV which was attached to a software of energy dispersive spectroscopy (EDS), to perform chemical microanalyses. SEM technique was also employed to perform punctual chemical analysis and X-ray mappings of elements in the un-milled and processed samples. X-ray diffraction technique was utilized in order to characterize the evolution of the crystal structure of the phases obtained during the mechanical milling process as a function of milling time. In order to perform this analysis a Siemens Diffractometer D500 was used, with the following working conditions, voltage of 30kV and a current of 20 mA. The specimens were scanned with a filter of CuK_α radiation with a wavelength of $\lambda = 1.5418 \text{ \AA}$ and using a step of $0.020^\circ / 0.6 \text{ sec.}$, in a range of 30° to 110° . The variation of crystallite size and lattice parameter of the phases obtained during the process of MA was also determined from X-ray Diffraction patterns.

3. Results and discussion

Fig. 1 a) and b) displays electron micrographs belonging to the metal powder particles of the Fe and Al, similarly Figure 1 c) shows the mixture of both elements in the un-milled condition. Figure 1 (a) exhibits particles with spherical morphology corresponding to Al (with a particle size distribution within the range of 2 to 14.9 μm) with approximate average size of 5 μm . Also, Figure 1 (b) shows larger particles that belongs to the Fe with irregular morphology with an approximate size within the range of 127 to 328 μm .

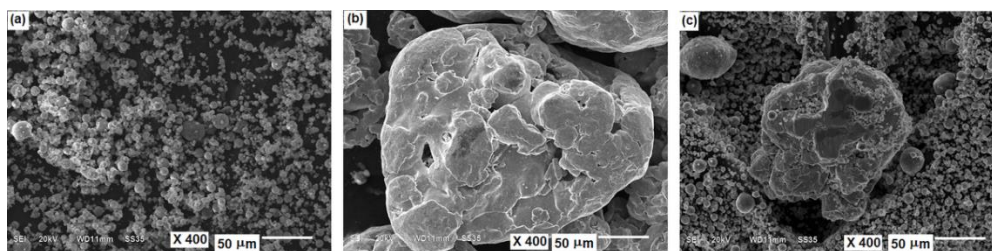


Fig. 1: Scanning electron micrographs of (a) Al, (b) Fe (c) a mixture of both Fe and Al.

Fig. 2 shows the microstructural evolution of the powder mixture particles milled up to 50 h with a ball weight / sample weight ratio of 4:1. Figure 2 (a) shows the microstructure of the sample at 20 h of milling, where it is observed that the particles of Al had a greater plastic deformation in comparison with Fe element, while at the 30 and 50 h of milling process, see Figures 2 (d) and 2 (g), a significant decrease in particle size is observed although agglomeration of powder particles is observed in this stages of the process. Also, figures 2 (b), (c), (e), (f), (h) and (i) displays the X-ray chemical mapping of Fe-Al powder mixture ball milled during 20, 30 and 50 h. In this micrographs a good chemical homogeneity of both Fe and Al is observed. Figure 3 shows the microstructural evolution of the powder mixture particles milled up to 50 h with a ball weight / sample weight ratio of 8:1. Figure 3 (a) shows the microstructure of the sample at 20 h of milling, where it is observed that the particles of Al had a greater plastic deformation in comparison with Fe, while at the 30 and 50 h of milling process (see Figures 3 (d) and 3 (g)), a significant decrease in particle size is observed although agglomeration of powder particles is observed in this stages of the process. Also, figures 3 (b), (c), (e), (f), (h) and (i) displays the X-ray chemical mapping of Fe-Al powder mixture ball milled during 20, 30 and 50 h. In this micrographs a good chemical homogeneity of both Fe and Al is observed. The reduction in particle size may be explained hereinafter in terms of the mechanism of the process of MA. During high energy milling the powder particles are flattened, cold welded, fractured and re-welded repeatedly. The particles are plastically deformed by the impact forces of the balls. In this way, causing work hardening and fracturing. Since in the initial stages of mechanical milling, the particles are soft (if combinations of brittle-ductile ductile-ductile material is used), its tendency to be welded together and form larger particles is high. With subsequent deformation induced by the milling process, the particles are hardened by mechanical working and fracture by a fatigue failure mechanism and / or by fragmentation of brittle flakes. The fragments generated by this mechanism may continue to decrease in size in the absence of strong forces that promote particle agglomeration [19]. Hongwei et al. [26] also reported a decrease in particle size with the course of time in a nanostructured FeAl intermetallic that were prepared directly by MA in a high-energy planetary ball-mill, in this case the ball-to powder weight ratio was about 20:1. The authors reported that particles were spherical after milling 50 h and the size of them was less than 30 nm.

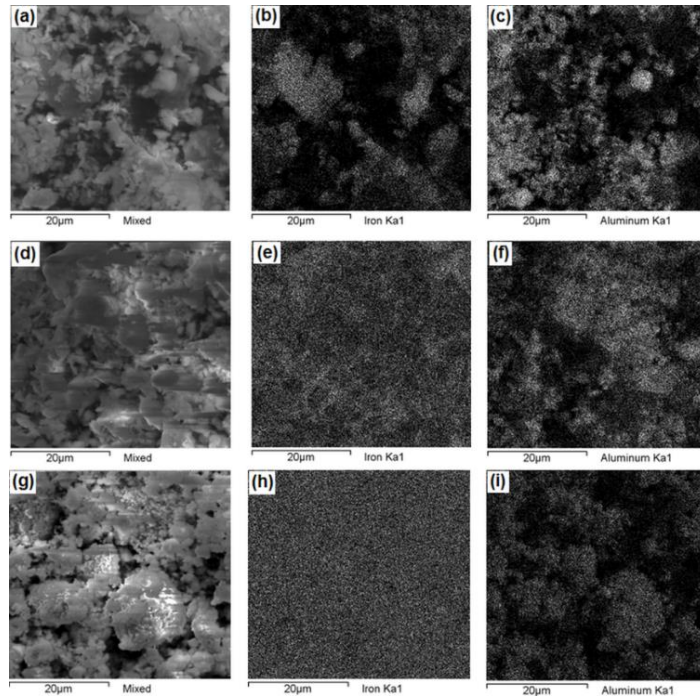


Figure 2 Secondary electron micrographs together with X-ray chemical mapping of Fe-Al powder mixture ball milled during 20 h, (a), (b) and (c), 30 h, (d), (e) and (f) and 50 h, (g), (h) and (i). The mechanical milling was performed in this case using a (powder weight / ball) ratio of 4:1.

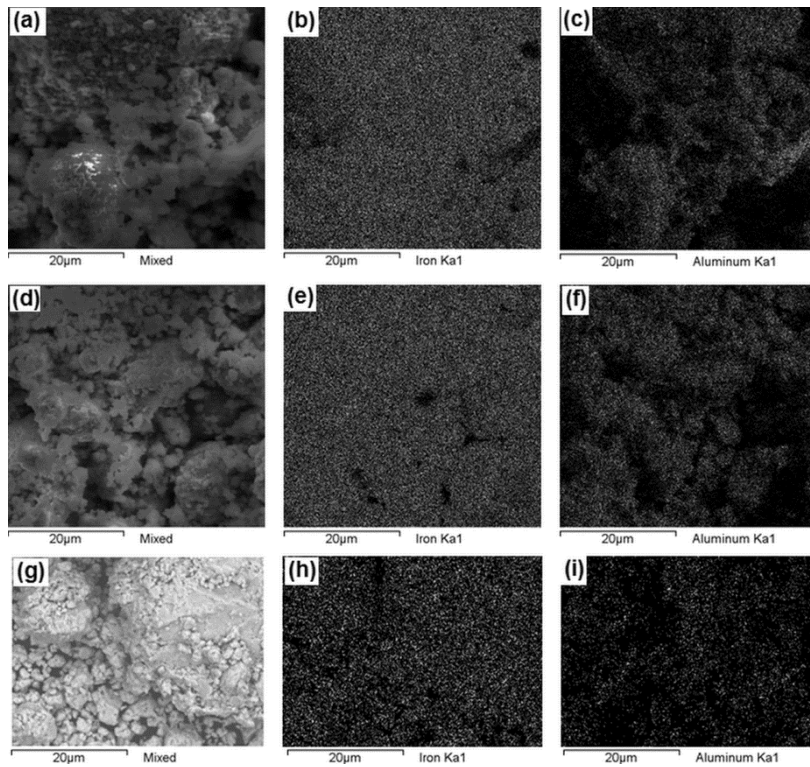


Figure 3 Secondary electron micrographs together with x-ray chemical mapping of Fe-Al powder mixture ball milled during 20 h, (a), (b) and (c); 30 h (d), (e) and (f) and 50 h (g), (h) and (i). The mechanical milling was performed in this case using a (powder weight / ball) ratio of 8:1.

Figure 4 (i) (a) displays the X-ray diffraction patterns of the un-milled sample, constituted by the mixture of Fe-Al elemental powders. Also illustrated in Figure 4 (i) - (b), (c) and (d), the X-ray diffraction patterns of the sample milled for 20, 30 and 50 h, in this case, it was used a (powder weight / balls weight) ratio of 4:1. The intensities of the diffraction peaks of Al located at about 38.6° and 78.4° was decreased while the milling time had elapsed. Also is observed that diffraction peak of Al at about 38.6° disappeared at 50 h of milling process. This findings revealed that at the milling times ≥ 10 h and minor to 50 h, a disordered solid solution α -FeAl together with the iron rich Fe phase were formed. However, at 50 h of milling process, only the existence of the disordered α -FeAl alloy was revealed. In addition, Figure 4 (ii) displays the X-ray diffraction of the highest Fe peak intensity. This illustration shows that diffraction peaks shift towards lower diffraction angles. This behavior can be associated to an increment of the solid solubility of Al in the α -FeAl phase [27] which in turn is reflected as a lattice parameter increment or decrement. Also, a diffraction peak broadening as the milling time elapsed is shown in Figure 4; the particular trend is associated in part to a decrease of crystallite size (or nano-sized grains).

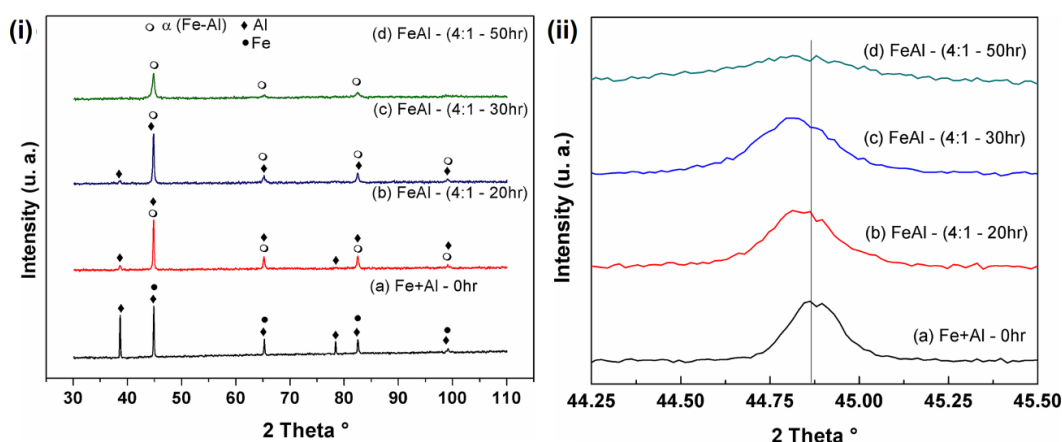


Fig. 4 (i) X-ray diffraction patterns of the powder mixture Fe40Al mechanically milled for various times using a (powder weight / balls weight) ratio of 4:1, (a) un-milled powder mixture, (b) milled at 20 h, (c) milled at 30 h and (d) milled at 50 h. (ii) Shift of the highest intensity diffraction Al peak, (a) un-milled powder mixture, (b) milled at 20 h, (c) milled at 30 h and (d) milled at 50 h.

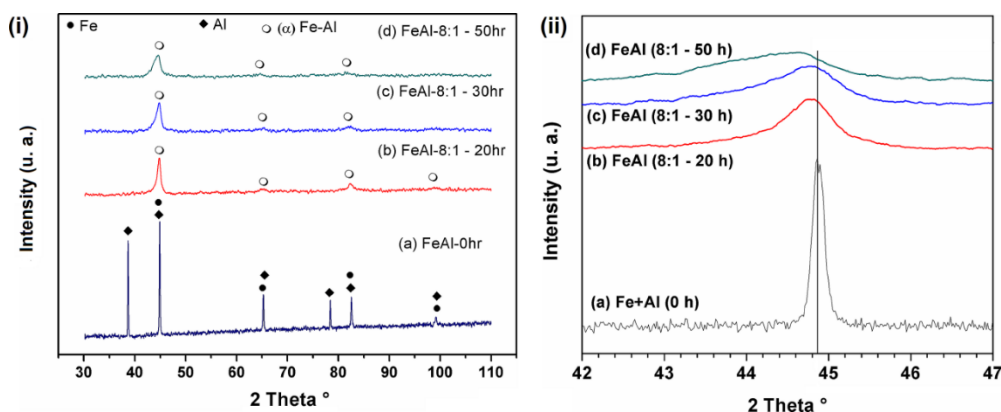


Fig. 5 (i) X-ray diffraction patterns of the powder mixture Fe40Al mechanically milled for various times using a (powder weight / balls weight) ratio of 8:1, (a) un-milled powder mixture, (b) milled at 20 h, (c) milled at 30 h and (d) milled at 50 h. (ii) Shift of the highest intensity diffraction Al + Fe peak, (a) un-milled powder mixture, (b) milled at 20 h, (c) milled at 30 h and (d) milled at 50 h.

Fig. 5 (i)a displays the X-ray diffraction profiles of the un-milled sample, constituted by the mixture of Fe-Al elemental powders. Also illustrated in Figure 5 (i)b, c and d, the X-ray diffraction patterns of the sample milled for 20, 30 and 50 h, in this case, it was used a (powder weight / balls weight) ratio of 8:1. The intensities of the diffraction peaks of Al located at about 38.6° and 78.4° was decreased while the milling time had elapsed. Also is observed that diffraction peak of Al at about 38.6° disappeared at 20 h of milling process. This findings revealed that at the milling times ≥ 20 h, a disordered solid solution α -FeAl was formed. In addition, Figure 5(ii) displays the X-ray diffraction of the highest Fe-Al peak intensity. This illustration shows that diffraction peaks shift towards lower diffraction angles. This behavior can be associated to an increment of the solid solubility of Al in the α -FeAl phase [19] which in turn is reflected as a lattice parameter increment or decrement. Vegard's law [28-29] establishes that the crystallographic parameters of a continuous substitutional solid solution varies linearly with concentration at constant temperature when the nature of the bonding is similar in the phases or constituents. This law has been widely used for calculating densities in solid solutions and to estimate the composition of solid solutions from diffraction data [30]. Besides, a diffraction peak broadening as the milling time elapsed is observed in Figure 5 ii. Where this trend is associated in part to a decrease of crystallite size (or nano-sized grains).

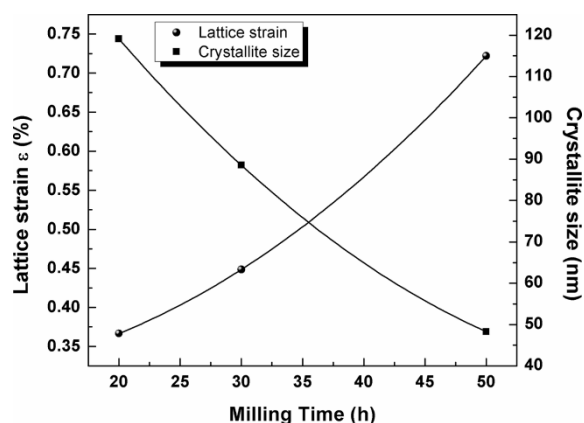


Fig. 6 Lattice strain ϵ (%) and crystallite size (nm) as a function of milling time for alloy Fe-Al milled by using a ball weight / powder weight ratio of 4:1.

Fig. 6 displays the dependence of both lattice strain and crystallite size with milling time, these values were determined from diffraction peaks belonging to the α -FeAl solid solution phase produced at 4:1 ratio. This illustration shows that crystallite size decreased with the lapse of milling time, whereas the lattice strain increased as the milling time increased from 20 to 50 h. Figure 6 exhibits that lattice strain increased from about 0.36 to 0.72 % when the milling time was increased from 20 to 50 h. In this case, it can be asseverated that the increment of lattice strain is originated by the transfer of mechanical energy provided by the repeating impacts of the milling balls with the metallic powders and the subsequent energy storage in form of crystal defects of the material being milled, where most of this energy is stored in form of dislocations. So, in this case, the broadening of diffraction peaks is due to a significant increment of dislocation density and a reduction of nano-sized grains with the lapse of milling time. Hongwei et al. [26] elaborated nanostructured FeAl intermetallics by mechanical alloying in a high-energy planetary ball-mill. In this case, elemental powders of composition Fe-50 at.% Al were mechanical alloyed using stainless steel vial and balls with diameter of about 20 mm. The ball-to-powder weight ratio was about 20:1. The authors reported a lattice strain increment from about 0.8 to 1.7 % while the milling time lapsed from 3 h to 50 h. In this case, the higher values of lattice strain (%) reported by Hongwei et al. [26] as compared with the reported in present work, are reasonable, since these authors elaborated the Fe50Al alloy with a high energy ball milling process, which can provide a higher level of mechanical energy as the process advanced. It is important to note that the dependence of the crystallite size or nano-sized grain (nm) with the milling time (h), in this case when the 4:1

ratio was used, can be represented by the second order polynomial function of equation (1), where “D” represents the crystallite size (nm) and “t” is the milling time (h).

$$D = 201.11 - 4.79t + 0.0348t^2 \quad (1)$$

Similarly, Figure 7 exhibits the dependence of both lattice strain and crystallite size with ball milling time, these values were determined from diffraction peaks belonging to the disordered α -FeAl solid solution phase produced at 8:1 ratio. This illustration shows that crystallite size decreased with the increase of milling time, while the lattice strain increased as the milling time elapsed from 20 to 50 h. The dislocation density increment induced by the ball milling process, induced in this case work hardening in powder particles which in turn favored the fracture process of powder particles. This behavior is reflected by the significant particle size diminution experienced by the disordered Fe-Al phase at 50 h of mechanical milling process, see Figure 3 g). It is worth noting that the dependence of the crystallite size (nm) with milling time (h), in this case when the 8:1 ratio was utilized, can be represented by second order polynomial function of equation (2), where D and t represent again the crystallite size (nm) and “t” is the milling time (h).

$$D = 45.11 - 0.569t + 0.00268t^2$$

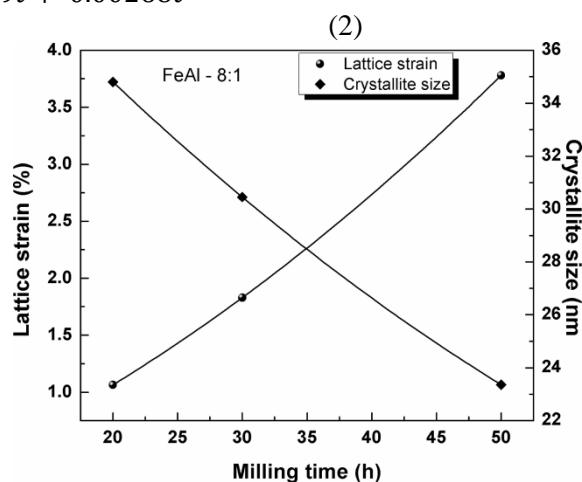


Fig. 7 Lattice strain ϵ (%) and crystallite size (nm) as a function of milling time for alloy Fe-Al milled by using a ball weight / powder weight of 8:1.

Reduction of crystallite size with milling time have been also observed previously. Wolski et al. [31], performed ball milling experiments in a powder mixture of Fe and Al with a chemical composition of Fe₄₀Al (at. %) by using a planetary ball mill at a rotational speed of 200 RPM and utilizing a ball weight / sample weight ratio of 50:1. The authors also reported a crystallite size reduction with the lapse of time. This behavior was related to the morphologic texture (sandwich microstructure obtained by MA) and also to a mechanism associated with the local melting of Aluminum. Figure 8 shows the variation of the lattice parameter obtained from the diffraction peaks corresponding to the disordered Fe₄₀Al alloy, (denoted as (α FeAl)) in the diffraction patterns of X-rays) in parallel way with the course of milling time. The tendency observed in the case of the condition of milling (8:1) shows an increase of lattice constant from 2.886 to 2.894 Å with the course of processing time.

Krasnowski and Kukik [32] subjected to a mechanical milling process a mixture of powders Fe₅₀Al (at.%) in a high energy mill SPEX 8000 with a (ball weight / sample weight) ratio of 8:1. The authors also reported an increase in lattice parameter with the lapse of time. This behavior may be due to two combined effects. In the first case, it can be explained in terms of the mechanism of formation of a solid solution, where the lattice parameter increment of the Fe₄₀Al phase is originated by the solution of Al atoms in the crystal lattice of Fe. In the second case, the increased lattice constant may be explained in terms of a process of ordering of the crystal structure, where the lattice parameter changes from low values to higher values. This trend

represents a disorder - order transition of Fe₄₀Al phase. The lattice parameter trend observed in this study has also been reported in previous researches. Haghghi et al. [33] subjected to mechanical milling a mixture of powders of initial composition Fe₅₀Al (% at.) in a planetary mill at 300 rpm, and the authors used a (ball weight / sample weight) ratio of 50:1 and stainless steel balls hardened. The authors reported an increase in lattice parameter of α -FeAl phase as the milling time progressed and this tendency was associated to the solution of Al atoms in the crystal lattice of Fe by these investigators.

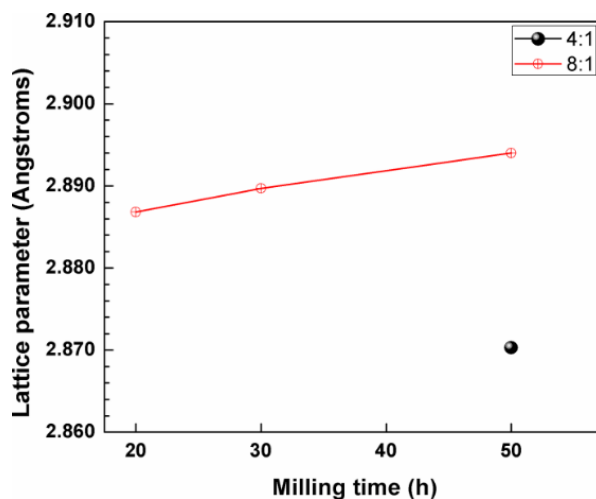


Fig. 8. Lattice parameter "a" (angstroms) as a function of milling time for alloy Fe-Al milled by using a ball weight / powder weight ratios of 8:1 and 4:1.

Better polynomial functions can be obtained by using a larger sample of points and more powerful methods as the generalized least squares method (GLQM), where the dependent variable y is a vector which is modeling by the next stochastic model depending of a β parameter which should be obtained [34]:

$$y = X\beta + \varepsilon \quad (3)$$

Where y is an $n \times 1$ vector, X is a full matrix $n \times m$ which elements are known and ε is a random vector. The advantage of using equation (3) is that different stochastic properties can be model in this way. For instance if the variance exhibits a heteroscedastic property (i.e. the variance is not constant in all the range of data), different regression models can be used. Nevertheless, for problems with different stochastic properties, GLQM should be adapted. A more practical solution is to determine the regression equation only using data sets of (y, x) points. In this case, y is usually the crystallite size and X has several columns where the data related to the mechanical alloying variables such milling time, the ball weight to powder weight ratio, the milling speed and milling time among others. Thus, regression methods using intelligent optimization have been devised, the more common methods are genetic algorithms and ant systems [35-37], and Neural Networks [38]. In these intelligent methods, usually two phases named learning and testing phase are applied. Firstly, a data set with known points (X, Y) are determined and "cleaned", which means that all the data are analyzed and filter of possible errors. Then, the data set is divided in two parts known as Learning and Test data; the proportion usually used is 80 and 20% respectively. Secondly, learning data are handled during the training phase by the algorithm (Genetic Algorithms, Neural Networks, and so on) in order to determine a regression model similar to equation (2). Then, the obtained regression model is tested during the testing phase using an accuracy measure, evaluating the model provided by the learning stage. In the case of big deviations, the learning stage is repeated modifying the algorithm parameters; for instance in [35] the number of generations were adjusted in order to tune the algorithm for better solutions than the classical ones. Because, intelligent optimization methods do not require particular mathematical foundations, they can be seen as black boxes were cleaning data and tuning process are usually the

requirements for many applications where the mechanical alloying technique was used to elaborate nano-crystalline alloys.

4. Conclusions

Particle size was significantly reduced during the course of milling. So, the particle size at different milling times resulted minor than particle size of the initial Fe elemental powders. When the balls to powder weight ratio of 8:1 had been utilized, a fully disordered alloy Fe₄₀Al had formed at 20 h of milling time. When the balls to powder weight ratio of 4:1 had been utilized, a fully disordered alloy Fe₄₀Al had formed at 50 h of milling time. The crystallite size corresponding to the disordered FeAl phase obtained in the process of AM decreased as time passed when both balls to powder weight ratio of (8:1 and 4:1) were used.

The lattice strain corresponding to the disordered FeAl phase obtained from diffraction peaks of XRD profiles increased as time passed when both balls to powder weight ratio of (8:1 and 4:1) were used. So, in this case, the lattice strain increment is due to a significant increment of dislocation density and a reduction of nano-sized grains with the lapse of milling time. The corresponding lattice parameter of the disordered alloy Fe₄₀Al increased with increasing milling time when a balls to powder weight ratio of 8:1 was used. This effect is due to a disorder-order transition when the crystal structure of the disordered solid solution Fe-Al (a) is transformed to a B2-type ordered crystal structure which pertain to Fe₄₀Al alloy.

References

- [1] T. Grosdidier, G. Ji, F. Bernard E. Gaffet, Z. A. Munir, S. Launois, *Intermetallics*, **14**(10-11), 1208 (2006).
- [2] E. Godlewska, S. Szczepanik, R. Mania, J. Krawiars and S. Kozinski *Intermetallics*, **11**(1-2) 307 (2003).
- [3] H. Skoghund, M. Wedel and K. Karlsson, *Intermetallics*, **12**(7-9), 977 (2004).
- [4] D. G. Morris, S. Gunther, *Materials Science and Engineering A* **208**(1), 7 (1996).
- [5] M. A. Morris, A. Dodge, D. G. Morris, *Nanostruct. Mater.* **11**(7), 873 (1999).
- [6] I. Baker & George E.P. *Aluminides: processing properties and the mechanical properties of FeAl: Proceedings of the international symposium on nickel and iron aluminides, British Library document; (pp. 145-155). 7-9 October 1996. Cincinnati, Ohio – USA. (1996).*
- [7] J. L. Jordan, S. C. Deevi, *Intermetallics*, **11**(6), 507 (2003).
- [8] A. Fraczkiewicz, A. S. Gay, M. Biscondi, *Materials Science and Engineering: A*, **258**(1), 108 (1998).
- [9] M. A. Crimp, K. Vedula, *Materials Science and Engineering*, **78**(2), 193 (1986).
- [10] M. A. Morris, A. Dodge, D. G. Morris, *Nanostructured Materials*, **11**(7), 873 (1999).
- [11] D. G. Morris & M. A. Morris-Munoz, *Intermetallics* **7**(10), 1121 (1999).
- [12] D. Kuc, G. Niewielski, M. Jabłońska, & I. Bednarczyk, *Journal of Achievements in Materials and Manufacturing Engineering*, **20**(s 143), 146 (2006).
- [13] M. Kupka, *Intermetallics*, **14**(2), 149 (2006).
- [14] M.A. Morris-Munoz, A. Dodge, D. G. Morris, *Nanostructured materials*, **11**(7), 873 (1999).
- [15] J. S. Benjamin, *Scientific American*, **234**(5), 40 (1976).
- [16] J. Kostrubanic, D. A. Koss, L. E. Locci & M. Nathal, M. (1990, January). On Improving the Fracture Toughness of a NiAl-Based Alloy by Mechanical Alloying. In *MRS proceedings* (Vol. 213, p. 679). Cambridge University Press.
- [17] J. S. Benjamin, M. J. Bomford, *Metallurgical Transactions A*, **8**(8), 1301 (1977).
- [18] B. S. Murty & S. Ranganathan, *International materials reviews*, **43**(3), 101 (1998).
- [19] C. Suryanarayana, *Progress in materials science*, **46**(1), 1 (2001).
- [20] M. Krasnowski, T. Kulik, *Intermetallics* **15**(2), 201 (2007).
- [21] S. Zhu, M. Tamura, K. Sakamoto, K. Iwasaki, *Materials Science and Engineering: A*, **292**(1), 83 (2000).

- [22] H. Shi, D. Guo, Y. Ouyang, *Journal of Alloys and Compounds*, **455**(1), 207 (2008).
- [23] M. Krasnowski, A. Grabias & T. Kulik, *Journal of alloys and compounds*, **424**(1), 119 (2006).
- [24] E. Jartych, *Journal of magnetism and magnetic materials*, **265**(2), 176 (2003).
- [25] F. Runhua, S. Kangning, Y. Yansheng, B. Zhichen, *Chinese Journal of Mechanical Engineering* **36**(8), 55 (2000).
- [26] S. Hongwei, G. Debo, O. Yifang, *Journal of Alloys and Compounds* **455**, 207 (2008).
- [27] C. Suryanarayana, E. Ivanov, V.V. Boldyrev, *Mater. Sci. Eng. A* **304-306**, 151 (2001).
- [28] L. Vegard, *Zeitschrift für Physik A Hadrons and Nuclei*, **5**(1), 17 (1921).
- [29] L. Vegard, *Zeitschrift für Kristallographie*, **67**(2), 239 (1928).
- [30] N. Nishiyama, J. Lin, A. Okazaki, M. Iwasaka, K. Hirakawa *Jap. J. Appl. Phys.* **29**, 369 (1990).
- [31] K. Wolski, G. Caerb, P. Delcroixb, R. Fillit, F. Thevenota, J. Cozea, *Materials Science and Engineering A*, **207**, 97 (1996).
- [32] M. Krasnowski, T. Kulik, *Materials Chemistry and Physics*, **116**(2), 631 (2009).
- [33] E. Haghghi, K. Janghorban, S. Izadi,, *Journal of Alloys and Compounds*, **495**, 260 (2010).
- [34] T. Kariya & H. Kurata, *Generalized Least Squares*, John Wiley and Sons, 2004.
- [35] C. Hernandez-Carreón, H. Huacuya, K.E. Espriella, G. Castilla Valdez, J. Tolama, *Advances in Soft Computing, Innovations in Hybrid Intelligent Systems*, Springer, **44**, 247 (2007).
- [36] M. Dorigo, M. Birattari & T. Stützle, "Ant colony optimization", *Computational Intelligence Magazine*, IEEE, **1**(4), 28 (2006).
- [37] M. Dorigo & T. Stützle, *Ant colony optimization: overview and recent advances*. In *Handbook of metaheuristics* (pp. 227-263). Springer US, (2010).
- [38] M. Abdellahi, H. Bahmanpour & M. Bahmanpour, *Ceramics International*, **40**(7), 9675 (2014).